Development 124, 2829-2841 (1997)
Printed in Great Britain © The Company of Biologists Limited 1997
DEV6293

Chimeric analysis of *fibroblast growth factor receptor-1* (*Fgfr1*) function: a role for FGFR1 in morphogenetic movement through the primitive streak

Brian G. Ciruna[1,2], Lois Schwartz[1], Kendraprasad Harpal[1], Terry P. Yamaguchi[1,*] and Janet Rossant[1,2,3,†]

[1]Samuel Lunenfeld Research Institute, Mount Sinai Hospital, 600 University Avenue, Toronto, Ontario, Canada M5G 1X5
[2]Department of Molecular and Medical Genetics, University of Toronto, Toronto, Ontario, Canada, M5S 1A8
[3]Department of Obstetrics and Gynecology, University of Toronto, Toronto, Ontario, Canada, M5S 1A8
*Present address: Department of Molecular and Cellular Biology, The Biological Laboratories, Harvard University, 16 Divinity Avenue, Cambridge, Massachusetts, 02138, USA

†Author for correspondence (e-mail: rossant@mshri.on.ca)

SUMMARY

Fibroblast growth factor (FGF) signaling has been implicated in the patterning of mesoderm and neural lineages during early vertebrate development. In the mouse, FGF receptor-1 (FGFR1) is expressed in an appropriate spatial and temporal manner to be orchestrating these functions. Mouse embryos homozygous for a mutated *Fgfr1* allele (*fgfr1*$^{\Delta tmk}$) die early in development, show abnormal growth and aberrant mesodermal patterning. We have performed a chimeric analysis to further study FGFR1 function in the morphogenesis and patterning of the mesodermal germ layer at gastrulation. At E9.5, *fgfr1*$^{\Delta tmk}$/*fgfr1*$^{\Delta tmk}$ cells showed a marked deficiency in their ability to contribute to the extra-embryonic, cephalic, heart, axial and paraxial mesoderm, and to the endoderm of chimeric embryos. Analysis at earlier stages of development revealed that *fgfr1*$^{\Delta tmk}$/*fgfr1*$^{\Delta tmk}$ cells accumulated within the primitive streak of chimeric embryos, and consequently failed to populate the anterior mesoderm and endodermal lineages at their inception. We suggest that the primary defect associated with the *fgfr1*$^{\Delta tmk}$ mutation is a deficiency in the ability of epiblast cells to traverse the primitive streak. *fgfr1*$^{\Delta tmk}$/*fgfr1*$^{\Delta tmk}$ cells that accumulated within the primitive streak of chimeric embryos tended to form secondary neural tubes. These secondary neural tubes were entirely *fgfr1*$^{\Delta tmk}$/*fgfr1*$^{\Delta tmk}$ cell derived. The adoption of ectopic neural fate suggests that normal morphogenetic movement through the streak is essential not only for proper mesodermal patterning but also for correct determination of mesodermal/neurectodermal cell fates.

Key words: receptor tyrosine kinase, gastrulation, primitive streak, mesoderm, FGF, mouse, chimera, neural tube

INTRODUCTION

Recently, much attention has been directed toward possible roles for FGF signaling in early vertebrate development, especially with respect to the patterning of early mesodermal and neural lineages. Studies in *Xenopus laevis* have provided compelling evidence that FGF signaling is directly involved in both of these processes. Exogenous basic FGF, when added to animal cap explants, is able to induce mesoderm from tissue normally fated to become ectoderm (Kimelman and Kirschner, 1987; Paterno et al., 1989; Slack et al., 1989). The introduction of a dominant negative FGF receptor into *Xenopus* embryos at various stages of development has demonstrated that FGF signaling is required for the expression of several early mesodermal markers, for the induction of posterior and ventral mesoderm, and for proper mesodermal maintenance during gastrulation (Amaya et al., 1991, 1993; Kroll and Amaya, 1996). Also, overexpression of embryonic FGF (eFGF) in *Xenopus* embryos has recently been shown to both upregulate and anteriorly extend the expression domains of posterior homeobox genes (Pownall et al., 1996). These and other recent findings which demonstrate that FGFs can induce posterior neural differentiation suggest that FGF signaling may be involved in the proper patterning of the developing anterior-posterior axis (Cox and Hemmati-Brivanlou, 1995; Kengaku and Okamoto, 1995; Lamb and Harland, 1995).

In mouse embryogenesis, mesoderm induction and patterning are thought to occur at gastrulation. The beginning of gastrulation is manifested by the formation of the primitive streak at the posterior end of the embryo. In a process of highly integrated cell and tissue movements, cells delaminate through the primitive streak and emerge between the epiblast and visceral endoderm to form the mesodermal germ layer. Fate-mapping of the mouse epiblast suggests that cells emerging from different anterior-posterior levels of the streak adopt different fates (Tam, 1989; Lawson et al., 1991; Beddington et al., 1992; Parameswaran and Tam, 1995). FGFs 3, 4, 5 and 8 are expressed within the primitive streak in spatial and temporal patterns which would be consistent with a role for FGF signaling in mesoderm induction or in regulating processes of fate determination (Wilkinson et al., 1988; Haub and Goldfarb, 1991; Niswander and Martin, 1992; Hebert et al., 1991).

Mutational analyses of *Fgf3* and *Fgf5* have failed to show defects in early gastrulation (Mansour et al., 1993; Hebert et al., 1994). The apparent 'expendable' nature of FGF3 and FGF5 function in early embryonic development is likely due to redundancy in FGF signaling as there is cross-specificity in ligand-receptor interactions (Ornitz et al., 1996), and local co-expression of other FGFs may therefore compensate for the early losses of function (Givol and Yayon, 1992). Targeted disruption of *Fgf4* results in abortive postimplantation development (Feldman et al., 1995). While this implicates a role for FGF4 in the survival and growth of the inner cell mass during postimplantation development, lethality occurs too early to address the role of FGF4 signaling in mesoderm induction and patterning.

Analysis of FGF function at the level of the receptor has proved more informative. *Fgfr1*, for example, is first expressed throughout the primitive ectoderm. In mid-streak staged embryos, *Fgfr1* expression is concentrated in the posterior mesoderm lateral to the primitive streak and is maintained in the migrating mesodermal wings; headfold stage embryos show strong expression in both neurectoderm and the developing paraxial and pre-somitic mesoderm (Orr-Urtreger et al., 1991; Yamaguchi et al., 1992). Thus, *Fgfr1* expression is consistent with a role for FGFs in mesoderm induction, neural induction, and somite formation and patterning. Targeted mutation of *Fgfr1* results in embryonic lethality between day 7.5 and 9.5 of development, with defects first manifesting themselves at the onset of gastrulation (Yamaguchi et al., 1994; Deng et al., 1994). Retarded development of homozygous *Fgfr1* mutant embryos suggests an early mitogenic role for FGFR1, and thickening of the posterior streak suggested that *Fgfr1* mutant cells were defective in migrating from the posterior primitive streak. Paraxial mesoderm of *Fgfr1* mutant embryos was much reduced, yet axial mesoderm was still present and possibly expanded, suggesting that FGFR1 may be involved in the allocation of progenitor cells among alternative pathways of mesoderm differentiation (Yamaguchi et al., 1994; Deng et al., 1994). Although it was clear that FGFR1 may play a role in mesodermal patterning and perhaps cell migration away from the posterior streak, the phenotype was complex and it was difficult to distinguish primary defects associated with the *Fgfr1* mutation from secondary defects resulting from grossly abnormal morphogenetic movements at gastrulation.

To further elucidate the primary modes of FGFR1 function, a chimeric analysis has been performed. A population of homozygous *fgfr1*$^{\Delta tmk}$ embryonic stem (ES) cells was established and aggregated with wild-type (WT) diploid morulae to generate chimeric embryos. Careful analysis of the behaviour and distribution of *fgfr1*$^{\Delta tmk}$*/fgfr1*$^{\Delta tmk}$ cells within chimeric embryos revealed that defects in mesodermal patterning may be secondary to an initial deficiency in the ability of mutant cells to traverse the primitive streak. The chimeric analysis also revealed that *Fgfr1* mutant cells which have accumulated in the streak display an inherent tendency to form secondary neural tubes. A role for FGFR1 in regulating the morphogenetic movements which are thought to mediate cell fate determination and lineage restriction at gastrulation, is discussed.

MATERIALS AND METHODS

ES cell isolation

The *fgfr1*$^{\Delta tmk}$ allele used in this study has been previously described (Yamaguchi et al., 1994). Briefly, exons 8-14 of the *Fgfr1* locus, which encode the transmembrane domain and most of the catalytic kinase domain, were replaced by homologous recombination with PGK*neo*; this should effectively eliminate catalytically active isoforms of the receptor. A second, independently derived mutation at the *Fgfr1* locus which truncated all major isoforms of the gene at the second extracellular immunoglobulin domain resulted in a similar mutant phenotype to that of *fgfr1*$^{\Delta tmk}$*/fgfr1*$^{\Delta tmk}$ embryos (Deng et al., 1994). Therefore, it is believed that both *Fgfr1* mutations are effectively null alleles.

To isolate ES cell lines homozygous for the *fgfr1*$^{\Delta tmk}$ mutation and marked with a ubiquitously expressed *lacZ* marker, *fgfr1*$^{\Delta tmk}$/+ mice (129 background) were first crossed with ROSA26 mice of a mixed background (Friedrich and Soriano, 1991). F_1 progeny were genotyped for the *Fgfr1* locus by PCR (Yamaguchi et al., 1994). *fgfr1*$^{\Delta tmk}$/+; ROSA26 *lacZ* +/– mice were intercrossed, and the day that vaginal plugs were detected was designated embryonic day 0.5 (E0.5). Blastocysts were flushed, with M2 medium, from the uterine horns of pregnant females at E3.5 (as described by Hogan et al., 1994), and zona pellucidae were removed by treatment with acid Tyrode's solution. Blastocysts were transferred to individual 10 mm wells containing a preformed feeder layer of mitotically inactivated fibroblasts and 1 ml of culture medium (Dulbecco's modified Eagle's medium [DMEM] supplemented with 100 μM non-essential amino acids, 1 mM sodium pyruvate, 1 μM β-mercaptoethanol, 2 mM L-glutamine, 15% fetal calf serum and 1× leukaemia inhibitory factor). Embryos were cultured at 37˚C, 5% CO_2 for 4-5 days to allow for inner cell mass (ICM) outgrowth. ICM outgrowths were then disaggregated into small, multi-cellular clumps by mouth pipetting with a series of finely drawn out Pasteur pipettes. Disaggregated outgrowths were cultured further until ES cell colonies developed. Colonies were picked and subcultured to establish cell lines. Cell lines were genotyped for the *Fgfr1* locus by Southern analysis (Yamaguchi et al., 1994) and the presence of the ROSA26 *lacZ* transgene was determined by β-galactosidase staining of ES cell colonies.

Generation of chimeric embryos

To assess the developmental potential of the ES cell lines generated, individual lines were aggregated with two tetraploid CD-1 embryos (Nagy et al., 1993). Previous studies have demonstrated that tetraploid cells do not contribute to fetal tissues of tetraploid embryo ↔ ES cell chimeras, therefore these chimeric embryos will be completely ES cell-derived (Nagy et al., 1993). Tetraploid CD-1 embryos were produced by the electrofusion of embryos at the two cell stage. Aggregates were transferred into the uteri of CD-1 foster mothers, chimeric embryos were dissected at early to mid-gestational stages, and developmental potential of each cell line assessed by gross phenotypic observation.

Diploid chimeric embryos were generated by aggregating an 8-10 cell clump of either *fgfr1*$^{\Delta tmk}$/+ or *fgfr1*$^{\Delta tmk}$*/fgfr1*$^{\Delta tmk}$ ES cells with CD-1 8-cell embryos, using the standard morulae aggregation technique (Nagy et al., 1993). Aggregates were transferred into the uteri of CD-1 foster mothers, chimeric embryos were dissected at early to mid-gestational stages, and the contribution of ES cells and CD-1 cells to the embryo was determined by whole-mount β-galactosidase staining.

β-gal staining of chimeric embryos

Embryos (or ES cells) were rinsed in 100 mM sodium phosphate pH 7.3, and then fixed in 0.2% gluteraldehyde, 2 mM $MgCl_2$, 5 mM EGTA, 100 mM sodium phosphate pH 7.3 at room temperature for 15-30 minutes depending on size of embryo (or 5 minutes for ES cells). Embryos were then washed 3 times in wash buffer at room temperature (0.02% NP-40, 0.01% deoxycholate, 2 mM $MgCl_2$, 100 mM sodium phosphate pH 7.3) for 15 minutes each (ES cells were washed 3× 5 minutes). Embryos or ES cells were stained in 1 mg/ml X-gal, 5 mM $K_3Fe(CN)_6$, 5 mM $K_4Fe(CN)_6$, 0.02% NP-40, 0.01% deoxycholate, 2 mM $MgCl_2$, 100 mM sodium phosphate pH7.3 at 37°C

overnight. Samples were then rinsed with wash buffer, rinsed in PBS, and postfixed overnight in 3.7% formaldehyde at 4°C.

After whole-mount β-galactosidase staining, chimeric embryos were photographed, dehydrated through an ethanol series and embedded in paraffin. Paraffin blocks were sectioned at 5 μm, sections were mounted onto glass slides, dewaxed and counterstained with Nuclear Fast Red.

Whole-mount RNA in situ hybridization

Whole-mount in situ hybridization was performed as described by Conlon and Rossant (1992). For sectioning of whole-mount stained embryos, specimens were postfixed in 3.7% formaldehyde overnight at 4°C. Embryos were embedded in paraffin, sectioned at 10 μm, mounted onto glass slides, dewaxed, and photographed using Nomarski optics.

The probes used for the whole-mount in situ hybridization studies were as follows: *Brachyury* (Herrmann, 1991), *Shh* (Echelard et al., 1993), *Sox-1* and *Sox-2* (unpublished, obtained from Robin Lovell-Badge), *Pax3* (Goulding et al., 1991), *Pax6* (Walther and Gruss, 1991), *mox-1* (Candia et al., 1992), *twist* (Wolf et al., 1991), and *snail* (Smith et al., 1992). The *Ncam* probe (obtained from Cynthia Faust) consisted of a 1 kb cDNA fragment spanning exons 3-9 (which contains nearly all IgG domains), cloned into the *Bam*HI site of pBS+ (Stratagene) phagemid vector.

RESULTS

Isolation of *lacZ* marked ES cell lines

ES cell lines were generated from the ICMs of blastocysts isolated from crosses of $fgfr1^{\Delta tmk}$/+; ROSA26 *lacZ*+/– animals (Fig. 1A). *lacZ* expression via the ROSA26 transgene is ubiquitous throughout early to mid gestational development (Friedrich and Soriano, 1991), and is therefore a useful marker of mutant cells in chimeric embryos.

From approximately 90 blastocysts cultured, 9 ES cell lines were recovered. It was expected that three-quarters of the isolated cell lines would be positive for *lacZ* expression (as determined by β-galactosidase staining), and that a quarter of the cell lines would be homozygous for the *Fgfr1* mutation. Southern blot analysis revealed that seven ES cell lines were homozygous for $fgfr1^{\Delta tmk}$, two cell lines were $fgfr1^{\Delta tmk}$/+, and that no +/+ cell lines were recovered (Fig. 1B,C). Therefore, in deriving ES cell lines from primary blastocyst cultures, there appeared to be a positive selection for $fgfr1^{\Delta tmk}/fgfr1^{\Delta tmk}$ cell lines. This selection for homozygous $fgfr1^{\Delta tmk}$ cells was statistically significant (P<0.005; Fig. 1C).

129 $fgfr1^{\Delta tmk}$/+ mice were initially crossed with ROSA26 mice of a mixed background before generating ES cell lines, therefore the $fgfr1^{\Delta tmk}$ allele was carried on a 129-derived chromosome. Since isolation of ES cells is more efficient on a 129 background (McWhir et al., 1996 and references therein), *Fgfr1* may be linked to a 129-specific polymorphism which promotes the maintenance, and hence derivation of $fgfr1^{\Delta tmk}/fgfr1^{\Delta tmk}$ ES cell lines. Another explanation for the positive selection of homozygous $fgfr1^{\Delta tmk}$ lines is that FGFR1 signaling may promote differentiation from a pluripotent state. In this case, $fgfr1^{\Delta tmk}/fgfr1^{\Delta tmk}$ ES progenitors would have a selective advantage in maintaining pluripotency and hence in being isolated as an undifferentiated cell line.

$fgfr1^{\Delta tmk}/fgfr1^{\Delta tmk}$ ↔ tetraploid CD-1 chimeras were generated using cell lines B2, C5B, C15 and A3, in order to assess the developmental potential of these cell lines. Tetraploid chimeras were examined at E8.5 and E9.5 of development. At E8.5, chimeras were developmentally delayed in comparison to similarly staged WT embryos. These embryos showed abnormal thickening of the posterior primitive streak, poorly developed head folds, an absence of somites, and ruffling of the extraembryonic endoderm. At E9.5, chimeras were poorly developed and showed an expanded midline, an absence of somites, small malformed head folds, and kinking of the posterior neural tube. All of these properties are characteristic of homozygous $fgfr1^{\Delta tmk}$ embryos (Yamaguchi et al., 1994), indicating that the developmental potential of the $fgfr1^{\Delta tmk}/fgfr1^{\Delta tmk}$ cell lines had not been altered. Furthermore,

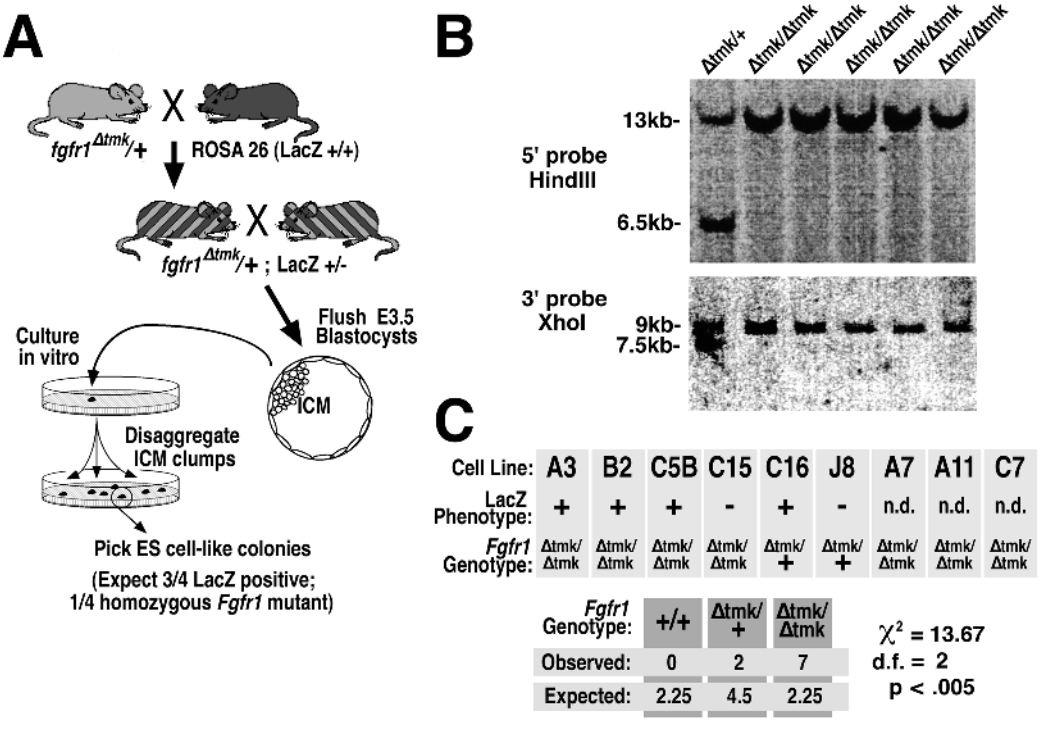

Fig. 1. Generation and characterization of ES cell lines. (A) Strategy for generating ES cell lines from primary blastocyst cultures. (B) Southern blot analysis of isolated ES cell lines; 5′ and 3′ *Fgfr1* probes were as previously described (Yamaguchi et al., 1994). (C) Summary of the *Fgfr1* genotypes and *lacZ* phenotypes of isolated ES cell lines.

it has been shown that the trophectoderm and primitive endoderm lineages of tetraploid embryo ↔ ES cell chimeras are strictly embryo-derived (Nagy et al., 1993). Since *fgfr1*$^{\Delta tmk}$/*fgfr1*$^{\Delta tmk}$ ↔ tetraploid CD-1 chimeras phenocopy homozygous *fgfr1*$^{\Delta tmk}$ embryos, then defects associated with the *fgfr1*$^{\Delta tmk}$ mutation are not caused by abnormal development of these tissues. Therefore, all defects observed in the *Fgfr1* homozygous mutant embryos can be explained by the abnormal development, morphogenesis and patterning of the extraembryonic mesoderm and definitive germ layers.

Cell lines B2 and C5B (which expressed the ROSA26 *lacZ* transgene) were used in subsequent diploid chimeric analyses. Since both cell lines produced similar results, data for these analyses have been pooled. Tetraploid aggregations were also performed with ES cell line C16 (*fgfr1*$^{\Delta tmk}$/+, *lacZ* positive) in order to test its pluripotency. Normal C16 derived embryos were recovered at E13.5, and therefore this *fgfr1*$^{\Delta tmk}$/+ cell line was used as a positive control in subsequent diploid chimeric analyses.

Whole-mount analysis of β-galactosidase stained chimeric embryos at E9.5 to E10.5

Diploid chimeric embryos were generated by aggregating approximately eight *fgfr1*$^{\Delta tmk}$/+ or *fgfr1*$^{\Delta tmk}$/*fgfr1*$^{\Delta tmk}$ ES cells with wild-type (WT) CD-1 embryos. At E9.5, *fgfr1*$^{\Delta tmk}$/+ ↔ CD-1 chimeras showed great variations in the extent of ES cell contribution to the embryo, with values ranging from <5% to 100% ES cell derived, as estimated by β-galactosidase staining (Fig. 2A,C,E). A similar range in ES contribution was observed in E9.5 *fgfr1*$^{\Delta tmk}$/*fgfr1*$^{\Delta tmk}$ ↔ CD-1 chimeras (Fig. 2B,D,F). This argues against a broad requirement for FGFR1 in early mitogenesis, since a major impairment in growth and proliferation would have been expected to reduce the overall contribution of *fgfr1*$^{\Delta tmk}$/*fgfr1*$^{\Delta tmk}$ cells to chimeric embryos.

Some phenotypically normal *fgfr1*$^{\Delta tmk}$/*fgfr1*$^{\Delta tmk}$ ↔ CD-1 chimeras were recovered at E10.5 (Fig. 3), indicating that WT cells could rescue the embryonic lethality and gastrulation defects associated with homozygous *fgfr1*$^{\Delta tmk}$ embryos. Viable chimeric embryos were also recovered at E16.5, however a complete analysis at late gestation was beyond the scope of this study. When the overall mutant cell contribution exceeded about 50%, *fgfr1*$^{\Delta tmk}$/*fgfr1*$^{\Delta tmk}$ ↔ CD-1 chimeric embryos developed gross phenotypic defects which ranged from apparent posterior neural tube duplications and ruffling of the dorsal ectoderm/neuroepithelium to posterior truncations, abnormal heart development, and failure in anterior neural tube closure (Fig. 3C-G). Similar defects were not observed in *fgfr1*$^{\Delta tmk}$/+ ↔ CD-1 chimeras (data not shown). Chimeric embryos that were completely *fgfr1*$^{\Delta tmk}$/*fgfr1*$^{\Delta tmk}$ cell derived phenocopied homozygous *fgfr1*$^{\Delta tmk}$ embryos (Fig. 2F).

Fgfr1 mutant cells show deficiencies in contributing to anterior mesoderm and endoderm lineages

Whole-mount β-galactosidase staining of *fgfr1*$^{\Delta tmk}$/*fgfr1*$^{\Delta tmk}$ ↔ CD-1 chimeric embryos revealed striking patterns in mutant cell dispersal: *fgfr1*$^{\Delta tmk}$/*fgfr1*$^{\Delta tmk}$ cells were deficient in contributing to the heart, and showed a strong tendency to accumulate within the tail of chimeric embryos (Figs 2D, 3A-C). To further investigate the distribution and behaviour of mutant cells within a chimeric background, 22 E9.5-10.5 *fgfr1*$^{\Delta tmk}$/*fgfr1*$^{\Delta tmk}$ ↔ CD-1 chimeric embryos, which showed varying degrees of ES-derived contribution, were histologically sectioned. All chimeras chosen appeared phenotypically normal, with the possible exception of posterior neural tube duplications. Fig. 4 depicts the level of ES cell contribution to various tissues of individual *fgfr1*$^{\Delta tmk}$/+ or *fgfr1*$^{\Delta tmk}$/*fgfr1*$^{\Delta tmk}$ ↔ CD-1 chimeric embryos. The anterior neural tube was used as a 'standard' for assessing the original ES-derived cell contribution to the epiblast since this tissue does not ingress through the primitive streak.

In *fgfr1*$^{\Delta tmk}$/*fgfr1*$^{\Delta tmk}$ ↔ CD-1 chimeric embryos, mutant cells contributed extensively to ectodermally derived tissues without causing gross morphological defects. The neural tube, surface ectoderm, and neural crest derivatives such as the branchial arches and dorsal root ganglia, were equally well populated by mutant cells (Figs 4, 5). Interestingly, *fgfr1*$^{\Delta tmk}$/*fgfr1*$^{\Delta tmk}$ cells showed a tendency to aggregate into distinct patches in the neuroepithelium and nasal placodes (Fig. 3E). The level of mutant cell contribution to the limb bud mesenchyme and lateral mesoderm of *fgfr1*$^{\Delta tmk}$/*fgfr1*$^{\Delta tmk}$ ↔ CD-1

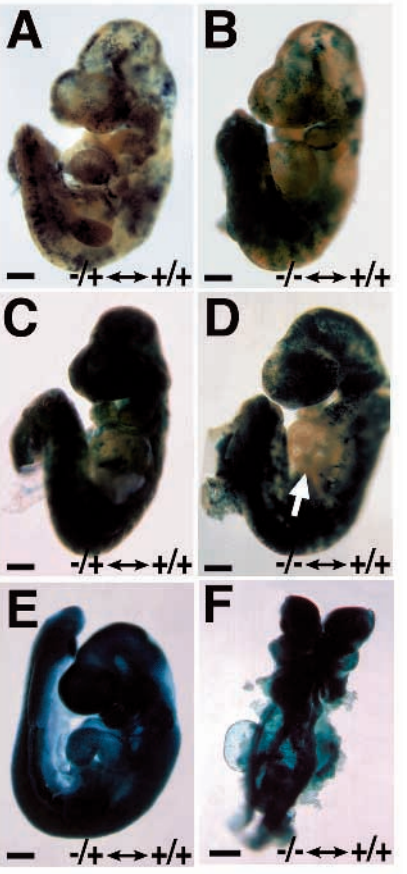

Fig. 2. Whole-mount analysis of ES-derived cell contribution to chimeric embryos at E9.5. *fgfr1*$^{\Delta tmk}$/*fgfr1*$^{\Delta tmk}$ or *fgfr1*$^{\Delta tmk}$/+ cells were visualized by β-galactosidase staining. *fgfr1*$^{\Delta tmk}$/+ ↔ CD-1 chimeras (A,C,E) and *fgfr1*$^{\Delta tmk}$/*fgfr1*$^{\Delta tmk}$ ↔ CD-1 chimeras (B,D,F) show similar ranges in ES-derived cell contribution. *fgfr1*$^{\Delta tmk}$/*fgfr1*$^{\Delta tmk}$ ↔ CD-1 chimeras show obvious deficiencies in mutant cell contribution to the heart (arrow in D). Chimeric embryos derived completely from *fgfr1*$^{\Delta tmk}$/+ cells appear phenotypically normal (E), while chimeras derived entirely from *fgfr1*$^{\Delta tmk}$/*fgfr1*$^{\Delta tmk}$ cells phenocopy homozygous *fgfr1*$^{\Delta tmk}$ embryos (F). Scale bars, 200 μm.

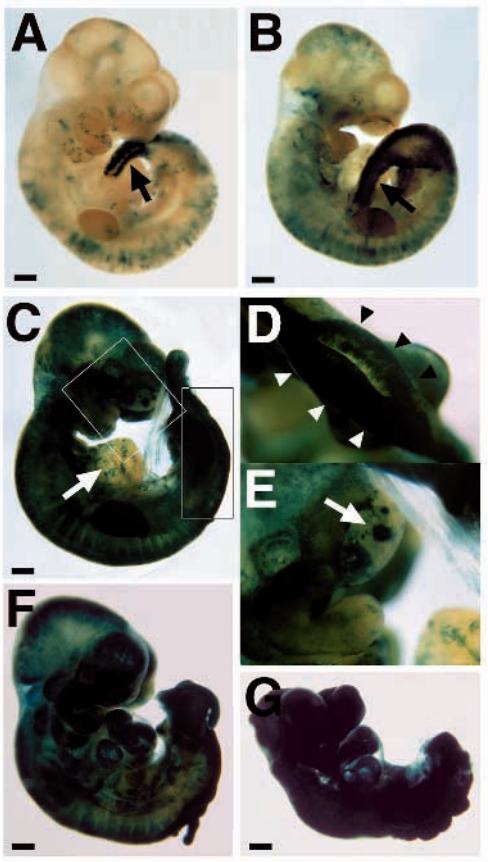

Fig. 3. Whole-mount analysis of β-galactosidase stained *fgfr1*$^{\Delta tmk}$/*fgfr1*$^{\Delta tmk}$ ↔ CD-1 chimeras at E10.5. (A,B) *fgfr1*$^{\Delta tmk}$/*fgfr1*$^{\Delta tmk}$ ↔ CD-1 chimeras with very low ES-derived cell contribution show caudal accumulations of *fgfr1*$^{\Delta tmk}$/*fgfr1*$^{\Delta tmk}$ cells (arrows) but are otherwise normal. (C,D,E) As the ES-derived cell contribution to chimeric embryos increases, deficiencies in *fgfr1*$^{\Delta tmk}$/*fgfr1*$^{\Delta tmk}$ contribution to the heart (arrow in C), apparent duplications of the posterior neural tube (arrowheads in D), and distinct aggregations of *fgfr1*$^{\Delta tmk}$/*fgfr1*$^{\Delta tmk}$ cells within nasal placode (arrow in E) become obvious. (F,G) Grossly abnormal embryos obtained when contribution of mutant cells exceed 50%. Scale bars, 200 μm.

chimeras was similar to that found in the neural tube, but *fgfr1*$^{\Delta tmk}$/*fgfr1*$^{\Delta tmk}$ cells appeared to accumulate in the mesenchyme of the tail (Figs 3A,B, 4).

In contrast, mutant cells were consistently under-represented in anterior mesoderm and endodermal lineages of *fgfr1*$^{\Delta tmk}$/*fgfr1*$^{\Delta tmk}$ ↔ CD-1 chimeric embryos (Fig. 4). Few mutant cells were observed in the cephalic, heart and somitic mesoderm populations (Fig. 5), and mutant cells were almost completely absent from the gut of *fgfr1*$^{\Delta tmk}$/*fgfr1*$^{\Delta tmk}$ ↔ CD-1 chimeras (Fig. 4). *fgfr1*$^{\Delta tmk}$/*fgfr1*$^{\Delta tmk}$ cells were also under-represented in the notochord of these chimeras, and contributed only to notochord of the posterior trunk and tail. Similar deficiencies in ES-derived contribution were not observed in *fgfr1*$^{\Delta tmk}$/+ ↔ CD-1 chimeras, although there was a slight bias against *fgfr1*$^{\Delta tmk}$/+ cell contribution to the endoderm (Fig. 4). This might indicate a dose-dependent requirement for FGFR1 in endoderm formation, or it may reflect an inherent bias against ES-derived contribution to the endoderm of ES cell ↔ embryo chimeras (see Discussion).

Several explanations exist for the observed deficiencies in *fgfr1*$^{\Delta tmk}$/*fgfr1*$^{\Delta tmk}$ cell contribution to the anterior mesoderm and endoderm of chimeric embryos. Mutant cells may have initially colonized these lineages, but either failed to proliferate, or underwent cell death. Alternatively, mutant cells may have been precluded from contributing to these lineages at the time of their inception at gastrulation. To differentiate between these possibilities, chimeric embryos were examined at earlier stages of development.

Fgfr1 mutant cells appear defective at traversing the primitive streak

Whole-mount β-galactosidase staining of early streak-stage *fgfr1*$^{\Delta tmk}$/+ ↔ CD-1 chimeric embryos demonstrated a random distribution of ES-derived cells. β-galactosidase staining appeared more intense in posterior-lateral portions of the embryo because of the extra cell layer formed by the advancing mesodermal wings (Fig. 6A,B). In contrast, *fgfr1*$^{\Delta tmk}$/*fgfr1*$^{\Delta tmk}$ ↔ CD-1 chimeras showed striking patterns in mutant cell distribution: *fgfr1*$^{\Delta tmk}$/*fgfr1*$^{\Delta tmk}$ cells accumulated along the primitive streak and were under-represented in the mesodermal wings, node and pre-chordal mesoderm (Fig. 6C,D). 20 E7.5 *fgfr1*$^{\Delta tmk}$/*fgfr1*$^{\Delta tmk}$ ↔ CD-1 chimeric embryos which showed a large range in ES-derived cell contribution (from <5% to 95%) were chosen for histological analysis.

Serial sections confirmed that *fgfr1*$^{\Delta tmk}$/*fgfr1*$^{\Delta tmk}$ cells were accumulating within the ectoderm and posterior mesenchyme of the primitive streak (Fig. 7). These *fgfr1*$^{\Delta tmk}$/*fgfr1*$^{\Delta tmk}$ accumulations could be observed even in those chimeras which showed only minimal (<5%) ES-derived cell contribution (Fig. 7A-C). In very strong *fgfr1*$^{\Delta tmk}$/*fgfr1*$^{\Delta tmk}$ ↔ CD-1 chimeras, patches of WT cells appeared to be selectively delaminating from an almost completely mutant epiblast layer (Fig. 7K,L). This suggests that *fgfr1*$^{\Delta tmk}$/*fgfr1*$^{\Delta tmk}$ cells were at a competitive disadvantage in traversing the primitive streak.

Although mutant cells contributed strongly to the epiblast of chimeric embryos, there was a striking deficit of *fgfr1*$^{\Delta tmk}$/*fgfr1*$^{\Delta tmk}$ cells in the mesodermal wings (Fig. 7D-F, G-I). This defect was not absolute; as the *fgfr1*$^{\Delta tmk}$/*fgfr1*$^{\Delta tmk}$ cell contribution increased, more mutant mesoderm cells were observed (Fig. 7G-I, J-L, M-O). *fgfr1*$^{\Delta tmk}$/*fgfr1*$^{\Delta tmk}$ mesodermal cells tended to accumulate along the posterior streak (Fig. 7I,L), giving the impression of the thickened streak characteristic of homozygous *fgfr1*$^{\Delta tmk}$ embryos. This mutant mesodermal population also appeared less able to migrate laterally around the embryo, since the leading edges of the mesodermal wings were composed largely of WT cells (Fig. 7K,O). Even in chimeras with over 95% *fgfr1*$^{\Delta tmk}$/*fgfr1*$^{\Delta tmk}$ cell contribution, WT cells formed the leading edge of the mesodermal wings; mutant cells accumulated within ‘pockets’ formed by abnormal buckling of the epiblast layer (Fig. 7O).

Fgfr1 mutant cells are defective in epithelial to mesenchymal transition at the primitive streak

Headfold to early somite-stage *fgfr1*$^{\Delta tmk}$/*fgfr1*$^{\Delta tmk}$ ↔ CD-1 chimeric embryos showed accumulations of mutant cells within the primitive streak and allantois (Fig. 6E,F). A deficiency in mutant cell contribution to the paraxial and presomitic mesoderm was also observed; similar trends were not observed

in the *fgfr1*$^{\Delta tmk}$/+ ↔ CD-1 chimeras (data not shown). 11 E8.5 *fgfr1*$^{\Delta tmk}$/*fgfr1*$^{\Delta tmk}$ ↔ CD-1 chimeras with varying degrees of mutant cell contribution (<5 to 70%) were histologically analyzed, and all showed a deficit of *fgfr1*$^{\Delta tmk}$/*fgfr1*$^{\Delta tmk}$ cells in the cephalic mesenchyme, heart primordia and paraxial mesoderm populations (Fig. 8). Even chimeras which had very high *fgfr1*$^{\Delta tmk}$/*fgfr1*$^{\Delta tmk}$ cell contribution to ectodermal lineages (60-70%) showed a near absence of mutant cells from anterior mesoderm (Fig. 8D). These chimeras appeared morphologically abnormal with kinked and misshapen neural folds.

fgfr1$^{\Delta tmk}$/*fgfr1*$^{\Delta tmk}$ ↔ CD-1 chimeric embryos with minimal (<5%) ES-derived cell contribution showed accumulations of mutant cells within the epiblast layer at the posterior streak (Fig. 8A-C). Mutant cells accumulated as a distinct 'block' of columnar epithelial cells, with WT cells forming mesenchyme on both sides of this accumulation (Fig. 8B). Also, in chimeras with high levels of ES-derived cell contribution, patches of WT cells could be seen delaminating from an almost entirely mutant epiblast layer (Fig. 8F,G). This suggests that *fgfr1*$^{\Delta tmk}$/*fgfr1*$^{\Delta tmk}$ cells are deficient in undergoing the epithelial to mesenchymal transition (EMT) which occurs at the streak. Despite apparent deficiencies in traversing the streak, *fgfr1*$^{\Delta tmk}$/*fgfr1*$^{\Delta tmk}$ cells contributed strongly to the mesoderm of more posterior regions of the embryo and mutant cells were well represented in lateral mesoderm. All *fgfr1*$^{\Delta tmk}$/*fgfr1*$^{\Delta tmk}$ ↔ CD-1 chimeras examined demonstrated strong ES-derived cell contribution to the allantois; the level of mutant cell contribution was highest at the base of the allantois and decreased distally (Fig. 6E,F). The remainder of the extra-embryonic mesoderm showed a striking deficiency in mutant cell colonization. *fgfr1*$^{\Delta tmk}$/*fgfr1*$^{\Delta tmk}$ cells were occasionally observed in the blood islands in the mesodermal component of the yolk sac, but only in blood islands situated along the posterior midline (not shown).

fgfr1$^{\Delta tmk}$/*fgfr1*$^{\Delta tmk}$ ↔ CD-1 chimeras form entirely mutant secondary neural tubes

At E9.5-10.5, *fgfr1*$^{\Delta tmk}$/*fgfr1*$^{\Delta tmk}$ ↔ CD-1 chimeras showed caudal accumulations of mutant cells. Histological sections through the tails of such chimeras revealed that *fgfr1*$^{\Delta tmk}$/*fgfr1*$^{\Delta tmk}$ cells appeared to form secondary neural tubes which were entirely mutant cell derived (Figs 5G, 9). 19 of the 22 *fgfr1*$^{\Delta tmk}$/*fgfr1*$^{\Delta tmk}$ ↔ CD-1 chimeras examined had developed these secondary

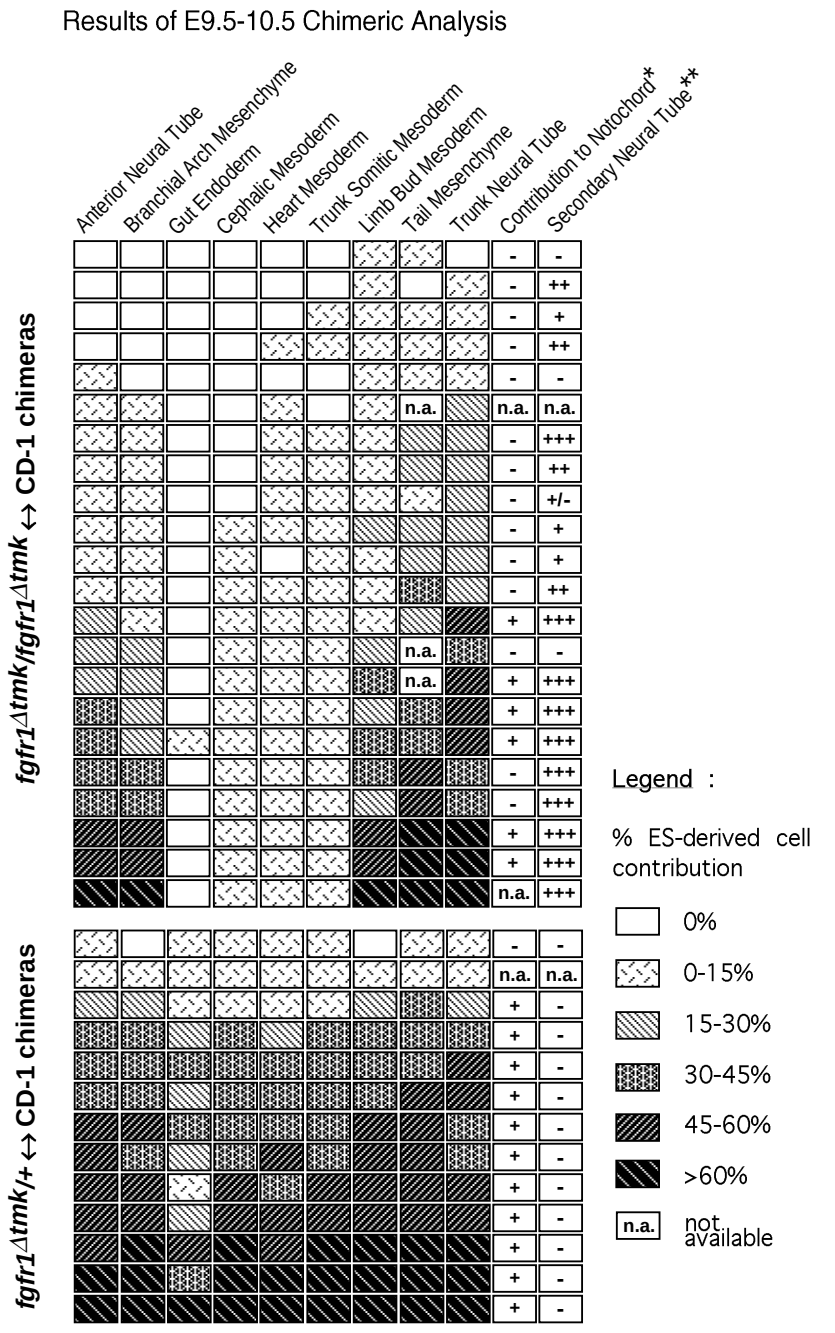

Fig. 4. Summary of the ES-derived cell contribution observed in various tissues of *fgfr1*$^{\Delta tmk}$/*fgfr1*$^{\Delta tmk}$ ↔ CD-1 (A) and *fgfr1*$^{\Delta tmk}$/+ ↔ CD-1 (B) chimeric embryos at E9.5 to E10.5. Chimeras chosen for analysis were phenotypically normal, with the possible exception of duplications in the posterior neural tube. The % ES-derived cell contribution to each lineage was estimated from histological sections on the basis of β-galactosidase staining. Each horizontal row depicts a different chimeric embryo; vertical columns represent the different tissues analyzed. *ES-derived cell contribution to the notochord is recorded only as present (+) or absent (–) owing to difficulties in scoring small tissue samples. **The presence of secondary neural tubes was scored as follows: (–) no secondary neural tube observed; (+/–) secondary neural tubes observed which ranged in size from small structures which pinched-off from the primary neural tube, to (+++) structures comparable to the primary neural tube in both size and form which extended caudally from the level of the hind limb bud.

structures (Fig. 4); of the 3 chimeras which did not, 2 displayed only minimal ES-derived cell contribution.

To rule out the possibility of β-galactosidase stain seeping into adjacent WT cells, thus masking their contribution to secondary neural tubes, an aggregation was performed between ROSA26 embryos and the C15 ES cell line (*fgfr1*$^{\Delta tmk}$/*fgfr1*$^{\Delta tmk}$; *lacZ* negative). In this case, secondary neural tubes did not show β-galactosidase staining, confirming that ectopic neural tubes were completely *fgfr1*$^{\Delta tmk}$/*fgfr1*$^{\Delta tmk}$ cell derived (data not shown).

Secondary neural tubes ranged in size from small structures which appeared to 'pinch off' from the primary neural tube (NT) in distal portions of the tail, to structures comparable in size to the primary NT, extending caudally from the hind limb bud level. The larger, secondary neural tubes originated from entirely *fgfr1*$^{\Delta tmk}$/*fgfr1*$^{\Delta tmk}$ cell-derived expansions of the neural plate (Fig. 9), and extended laterally from the central neural groove. These ectopic neural plates were excluded from primary NT closure, and folded separately into secondary neural tubes (Fig. 9).

To verify the neural identity of these ectopic tubes, whole-mount RNA in situs were performed using *Sox-1*, *Sox-2* and *Ncam* probes. *Sox-1* and *Sox-2* are SRY related genes; *Sox-1* expression is restricted to neurectodermal lineages, and *Sox-2* is initially expressed throughout the ectoderm and is later restricted to neuroepithelia (Collignon et al., 1996). Both *Sox-1* (Fig. 10A) and *Sox-2* (data not shown) were expressed in the primary and secondary neural tubes. NCAM, a neural cell adhesion molecule, was also expressed in both secondary and primary neural tubes, and showed normal expression in the surrounding somitic mesoderm (Fig. 10B). In situs were also performed using *mox-1*, *twist*, *snail* and *Brachyury* probes to ensure that the secondary neural tubes demonstrated no elements of mesodermal identity; mesoderm marker expression was not observed (not shown). Secondary neural tubes were often surrounded by ill-defined *fgfr1*$^{\Delta tmk}$/*fgfr1*$^{\Delta tmk}$ mesenchymal tissue (Fig. 9); the pattern of *mox-1* expression in the tails of chimeric embryos suggests that this poorly organized mesenchymal tissue has paraxial mesoderm identity (Fig. 10E). Lack of *Brachyury* staining associated with the secondary NT verified histological analyses which showed that secondary notochords were not associated with the ectopic neural tubes. Dorsal-ventral patterning of the secondary NT was also examined with *Pax3* and *Pax6*, and *shh* probes. As expected, the secondary neural tubes, which lacked notochords, did not show floor plate expression of *shh* (data not shown). *Pax3* is normally expressed in the dermamyotome and dorsal neural tube; *Pax6* expression is restricted to lateral walls of the neural tube. Both *Pax6* and *Pax3* appeared to be expressed in their proper domains (Fig. 10C and D, respectively).

DISCUSSION

Chimeric analysis has furthered our understanding of the developmental processes affected by the *fgfr1*$^{\Delta tmk}$ mutation. *fgfr1*$^{\Delta tmk}$/*fgfr1*$^{\Delta tmk}$ ↔ tetraploid CD-1 aggregations demonstrated unequivocally that defects associated with the mutated *Fgfr1* allele are intrinsic to definitive embryonic germ layers and to the extra-embryonic mesoderm. In *fgfr1*$^{\Delta tmk}$/*fgfr1*$^{\Delta tmk}$ ↔ diploid CD-1 chimeras, mutant cells contributed strongly to ectodermal lineages, and this argues against an early role for FGFR1 signaling in the development of the ectoderm and

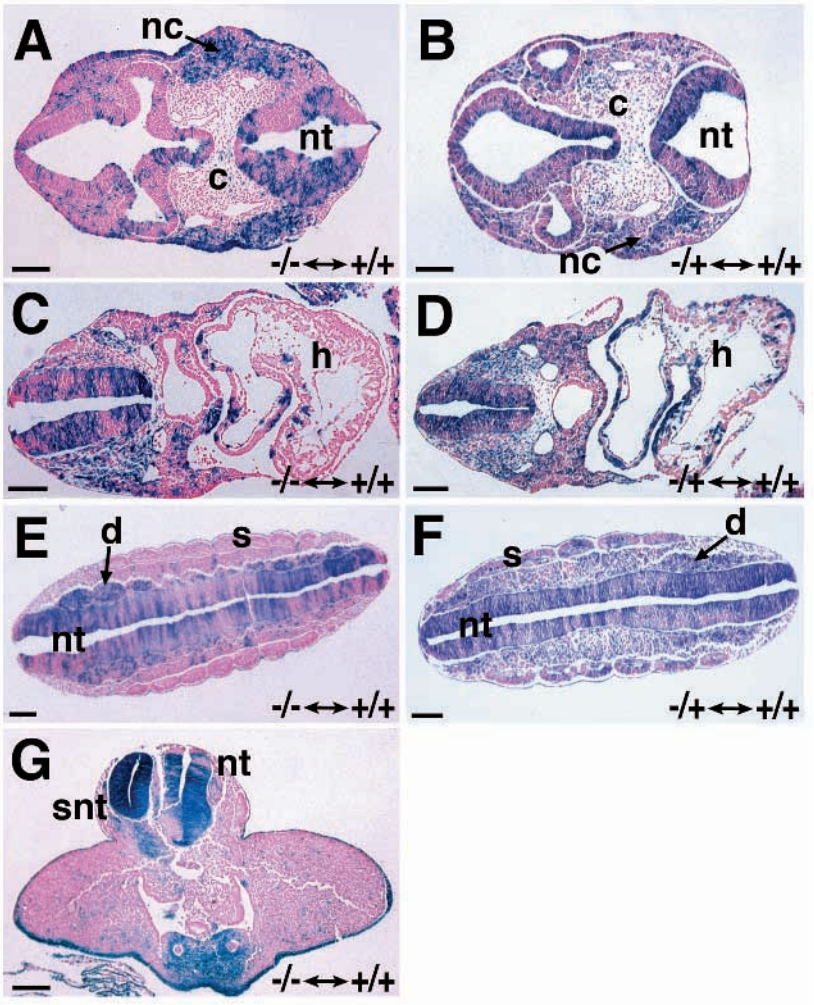

Fig. 5. Histological analysis of whole-mount β-galactosidase stained chimeric embryos at E9.5. (A,B) Sections through the head of matched *fgfr1*$^{\Delta tmk}$/*fgfr1*$^{\Delta tmk}$ ↔ CD-1 (A) and *fgfr1*$^{\Delta tmk}$/+ ↔ CD-1 (B) chimeric embryos show a relative deficiency in *fgfr1*$^{\Delta tmk}$/*fgfr1*$^{\Delta tmk}$ cell contribution to cephalic mesenchyme. (C,D) *fgfr1*$^{\Delta tmk}$/*fgfr1*$^{\Delta tmk}$ cell contribution to the heart of chimeric embryos (C) is deficient compared to ES-derived contribution to the heart of a matched *fgfr1*$^{\Delta tmk}$/+ ↔ CD-1 chimera (D). (E,F) Sections through the trunk of matched *fgfr1*$^{\Delta tmk}$/*fgfr1*$^{\Delta tmk}$ ↔ CD-1 (E) and *fgfr1*$^{\Delta tmk}$/+ ↔ CD-1 (F) chimeric embryos show strong deficiencies in *fgfr1*$^{\Delta tmk}$/*fgfr1*$^{\Delta tmk}$ cell contribution to somitic mesoderm. (G) *fgfr1*$^{\Delta tmk}$/*fgfr1*$^{\Delta tmk}$ ↔ CD-1 chimeras commonly form secondary neural tubes through their posterior trunk and tail; secondary neural tubes are entirely *fgfr1*$^{\Delta tmk}$/*fgfr1*$^{\Delta tmk}$ cell derived. Neural tube (nt), neural crest (nc), cephalic mesenchyme (c), heart (h), dorsal root ganglion (d), somitic mesoderm (s), secondary neural tube (snt). Scale bars, 100 μm.

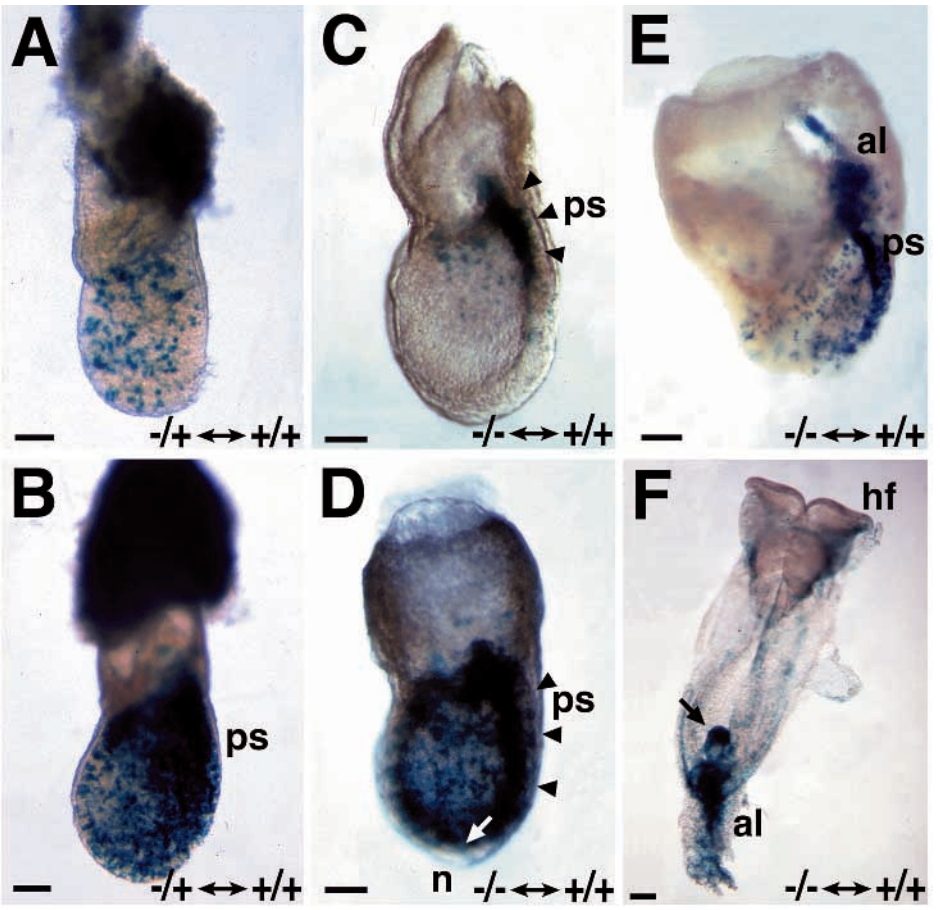

Fig. 6. Whole-mount analysis of β-galactosidase stained chimeric embryos at E7.5 to E8.5. (A) Early streak-stage and (B) mid streak-stage *fgfr1*$^{\Delta tmk}$/+ ↔ CD-1 chimeras showing that *fgfr1*$^{\Delta tmk}$/+ cells are randomly distributed throughout the embryo. Note the intense posteriolateral β-galactosidase staining which corresponds to the advancing mesodermal wings (B); anterior is to the left. (C,D) E7.5 *fgfr1*$^{\Delta tmk}$/*fgfr1*$^{\Delta tmk}$ ↔ CD-1 chimeras showing an accumulation of *fgfr1*$^{\Delta tmk}$/*fgfr1*$^{\Delta tmk}$ cells along the posterior streak; anterior is to the left. Note the deficiency of *fgfr1*$^{\Delta tmk}$/*fgfr1*$^{\Delta tmk}$ cell contribution to the node and pre-chordal mesoderm (arrow in D), and to the mesodermal wings. (E,F) *fgfr1*$^{\Delta tmk}$/*fgfr1*$^{\Delta tmk}$ ↔ CD-1 chimeras at E8.0 (E), and at E8.5 (F) showing continued accumulation of *fgfr1*$^{\Delta tmk}$/*fgfr1*$^{\Delta tmk}$ cells along the primitive streak, and within the allantois. Note the distinct accumulation of mutant cells within the primitive ectoderm of the posterior streak (arrow in F). Primitive streak (ps), node (n), allantois (al), head fold (hf). Scale bars, 50 μm (A-D), 100 μm (E-F).

its derivatives. Furthermore, since the epiblasts of *fgfr1*$^{\Delta tmk}$/+ and *fgfr1*$^{\Delta tmk}$/*fgfr1*$^{\Delta tmk}$ ↔ CD-1 chimeras showed similar ranges in ES-derived cell contribution, this argues against a strong mitogenic role for FGFR1 in early development (although a specific role in mesoderm proliferation cannot be completely discounted).

The primary defect associated with the *Fgfr1* mutation is a deficiency in traversing the primitive streak

This study has also provided further insight into the role of FGFR1 in the morphogenesis and patterning of mesoderm at gastrulation. *fgfr1*$^{\Delta tmk}$/*fgfr1*$^{\Delta tmk}$ ↔ CD-1 chimeras demonstrated strong deficiencies in the ability of mutant cells to populate not only the paraxial mesoderm (as already observed in the mutant analyses), but also the extra-embryonic, cephalic, heart and axial mesoderm, plus the endodermal lineages of E9.5-10.5 chimeric embryos. Some mutant cells were found in all lineages, and this confirms previous studies into the differentiation capacity of FGFR1 deficient ES cell lines as teratomas, which suggested that FGFR1 is not required in a cell-autonomous manner for cell fate specification (Deng et al., 1994). Rather, the chimeric analysis suggests that FGFR1 is required for correct morphogenetic movement of mesodermal progenitor cells through the primitive streak at gastrulation. In *fgfr1*$^{\Delta tmk}$/*fgfr1*$^{\Delta tmk}$ ↔ CD-1 chimeras, *fgfr1*$^{\Delta tmk}$/*fgfr1*$^{\Delta tmk}$ cells are deficient at traversing the primitive streak. *Fgfr1* mutant cells accumulate along the posterior midline and consequently fail to populate the mesodermal wings which have been identified as the source of presumptive extra-embryonic, heart and cephalic mesoderm (Parameswaran and Tam, 1995).

Axial and paraxial mesoderm are thought to be produced from stem-cell populations residing within the node and anterior portions of the primitive streak (Beddington, 1994; Tam and Beddington, 1987; Lawson et al., 1991; Nicolas et al., 1996). These progenitor populations form early in gastrulation, after extra-embryonic, cephalic and heart mesoderm progenitors have exited the streak (Lawson et al., 1991). Since *fgfr1*$^{\Delta tmk}$/*fgfr1*$^{\Delta tmk}$ cells appear to be defective at delaminating from the primitive streak, and since chimeric embryos show deficiencies in mutant cell colonization of the node, prechordal and early paraxial mesoderm populations, we suggest that *fgfr1*$^{\Delta tmk}$/*fgfr1*$^{\Delta tmk}$ cells were out-competed by WT cells in populating the axial and paraxial progenitor populations early in gastrulation. Interestingly, the resurgence of mutant cells within the posterior notochord may indicate later recruitment of *fgfr1*$^{\Delta tmk}$/*fgfr1*$^{\Delta tmk}$ cells to the axial progenitor pool over the course of gastrulation.

Definitive endoderm is also derived from epiblast cells which have delaminated at or near the anterior end of the early primitive streak (Lawson et al., 1991). Since *fgfr1*$^{\Delta tmk}$/*fgfr1*$^{\Delta tmk}$ cells are defective in traversing the streak, it is perhaps not surprising that there was a near absence of mutant cells in the gut of *fgfr1*$^{\Delta tmk}$/*fgfr1*$^{\Delta tmk}$ ↔ CD-1 chimeric embryos. Slight

deficiencies in ES-derived contribution to the endoderm were also observed in *fgfr1*$^{\Delta tmk}$/+ ↔ CD-1 chimeric embryos. This selection against *fgfr1*$^{\Delta tmk}$/+ cell contribution to the endodermal lineage may reflect an inherent bias in the distribution of 129 ES-progenitors within 129 ES cell ↔ CD-1 chimeras. The results of other chimeric analyses in our lab have shown that such biases against ES-derived cell contribution to endoderm exist independently of the *Fgfr1* genotype (unpublished lab observations).

In contrast to the anterior mesoderm and endodermal populations, the limb bud, lateral mesoderm and allantois of chimeric embryos were well colonized by *fgfr1*$^{\Delta tmk}$/*fgfr1*$^{\Delta tmk}$ cells. Thus, mutant cells were ultimately able to traverse the posterior streak. This skewed distribution of *fgfr1*$^{\Delta tmk}$/*fgfr1*$^{\Delta tmk}$ mesoderm might indicate a differential requirement for FGFR1 at various A-P levels of the primitive streak. *Fgf4* and *Fgf5* are expressed predominantly within the anterior two-thirds of the egg cylinder and streak (Haub and Goldfarb, 1991; Niswander and Martin, 1992; Hebert et al., 1991) and could therefore be responsible for anterior streak-specific FGFR1 signaling. However, *fgfr1*$^{\Delta tmk}$/*fgfr1*$^{\Delta tmk}$ cells were still observed accumulating within the epiblast and mesenchyme of the posterior streak. Thus, the fact that more mutant cells successfully traversed this portion of the streak may simply reflect the 'competitive' nature of the chimeric analysis: over the course of gastrulation, WT cells preferentially exited and *fgfr1*$^{\Delta tmk}$/*fgfr1*$^{\Delta tmk}$ cells progressively accumulated within the streak. Eventually, *Fgfr1* mutant cells constituted the majority of the mesodermal progenitor population, and were therefore forced to contribute to 'posterior' mesoderm lineages.

This competitive nature of the chimeric analysis might also explain differences observed in the behaviour and patterning of *fgfr1*$^{\Delta tmk}$/*fgfr1*$^{\Delta tmk}$ mesodermal progenitors between homozygous mutant and chimeric embryos. Although cephalic, heart and axial mesoderm were produced in homozygous *fgfr1*$^{\Delta tmk}$ embryos, these lineages were poorly colonized by mutant cells in *fgfr1*$^{\Delta tmk}$/*fgfr1*$^{\Delta tmk}$ ↔ CD-1 chimeras where WT cells demonstrated a competitive advantage in traversing the streak. Therefore, while the homozygous mutant analyses indicate a specific role for

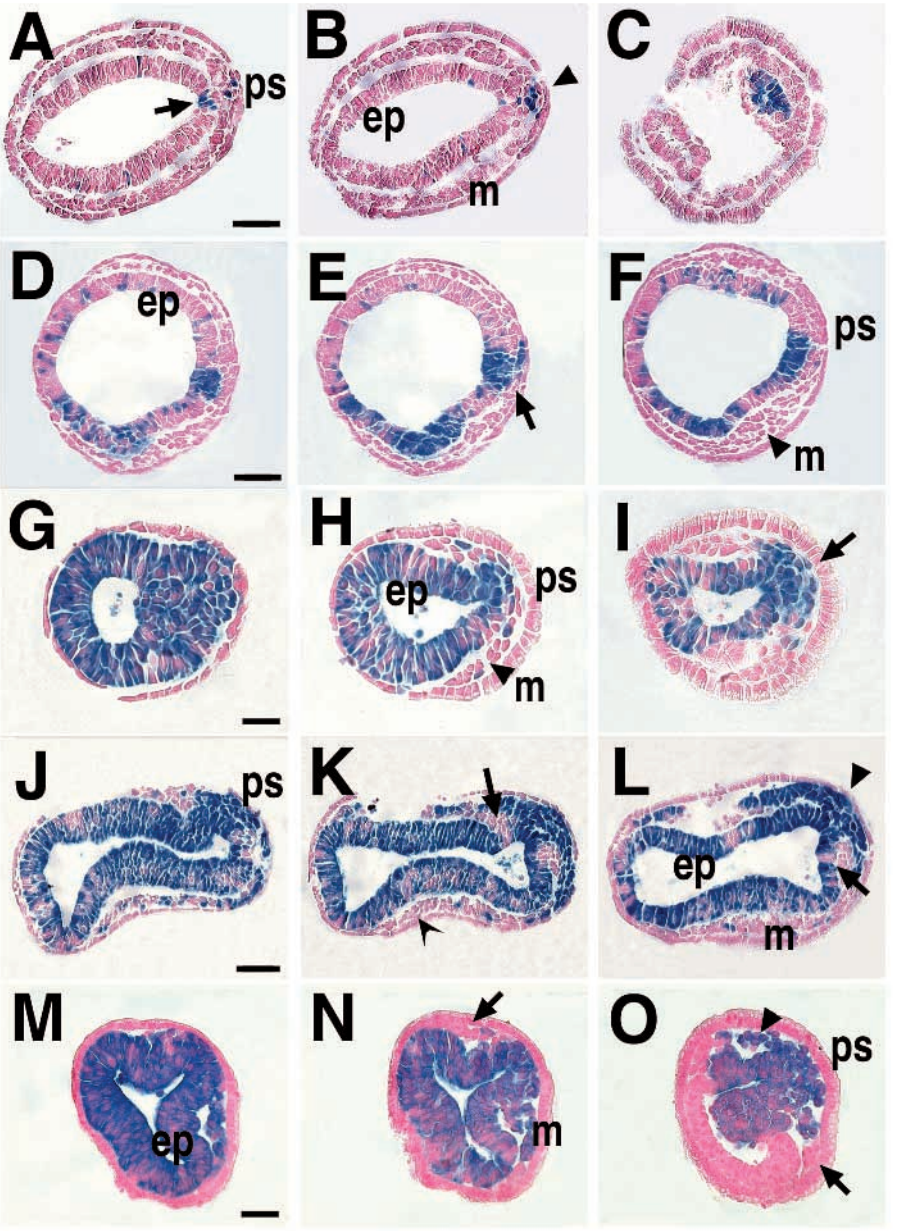

Fig. 7. Histological analysis of whole-mount β-galactosidase stained *fgfr1*$^{\Delta tmk}$/*fgfr1*$^{\Delta tmk}$ ↔ CD-1 chimeras at E7.5; primitive streak is to the right. Distal to more proximal transverse sections through five *fgfr1*$^{\Delta tmk}$/*fgfr1*$^{\Delta tmk}$ ↔ CD-1 chimeras are shown; ES-derived cell contribution to the distal epiblast was approximately 5% (A-C), 30% (D-F), 80% (G-I) and 95% (J-L, and M-O). (A-C) Chimeric embryos with minimal ES-derived cell contribution show accumulations of *fgfr1*$^{\Delta tmk}$/*fgfr1*$^{\Delta tmk}$ cells within the epiblast (arrow) and mesenchyme (arrowhead) of the posterior streak. (D-F) Stronger chimeras continue to show accumulations of *fgfr1*$^{\Delta tmk}$/*fgfr1*$^{\Delta tmk}$ cells along the posterior midline (arrow); mutant cells are deficient at contributing to the mesodermal wings (arrowhead) when compared with ES-derived cell contribution to the epiblast layer. (G-I) The deficit of *fgfr1*$^{\Delta tmk}$/*fgfr1*$^{\Delta tmk}$ mesodermal cells is quite pronounced in very strong chimeric embryos (arrowhead); mutant cells accumulate within the mesenchyme of the posterior primitive streak (arrow). (J-L) In chimeras which are almost completely *fgfr1*$^{\Delta tmk}$/*fgfr1*$^{\Delta tmk}$ cell derived, WT cells appear to selectively delaminate from the primitive streak (arrows). *fgfr1*$^{\Delta tmk}$/*fgfr1*$^{\Delta tmk}$ mesodermal cells accumulate beneath the primitive streak (arrowhead) while the leading edge of the mesodermal wings is composed largely of WT cells (chevron). (M-O) Another almost completely *fgfr1*$^{\Delta tmk}$/*fgfr1*$^{\Delta tmk}$ cell-derived chimera showing WT cells at the leading edge of the mesodermal wings (arrows), and mutant cells accumulating within 'pockets' formed from abnormal folding of the epiblast layer (arrowhead). Primitive streak (ps), epiblast (ep), mesodermal wings (m). Scale bars, 50 μm.

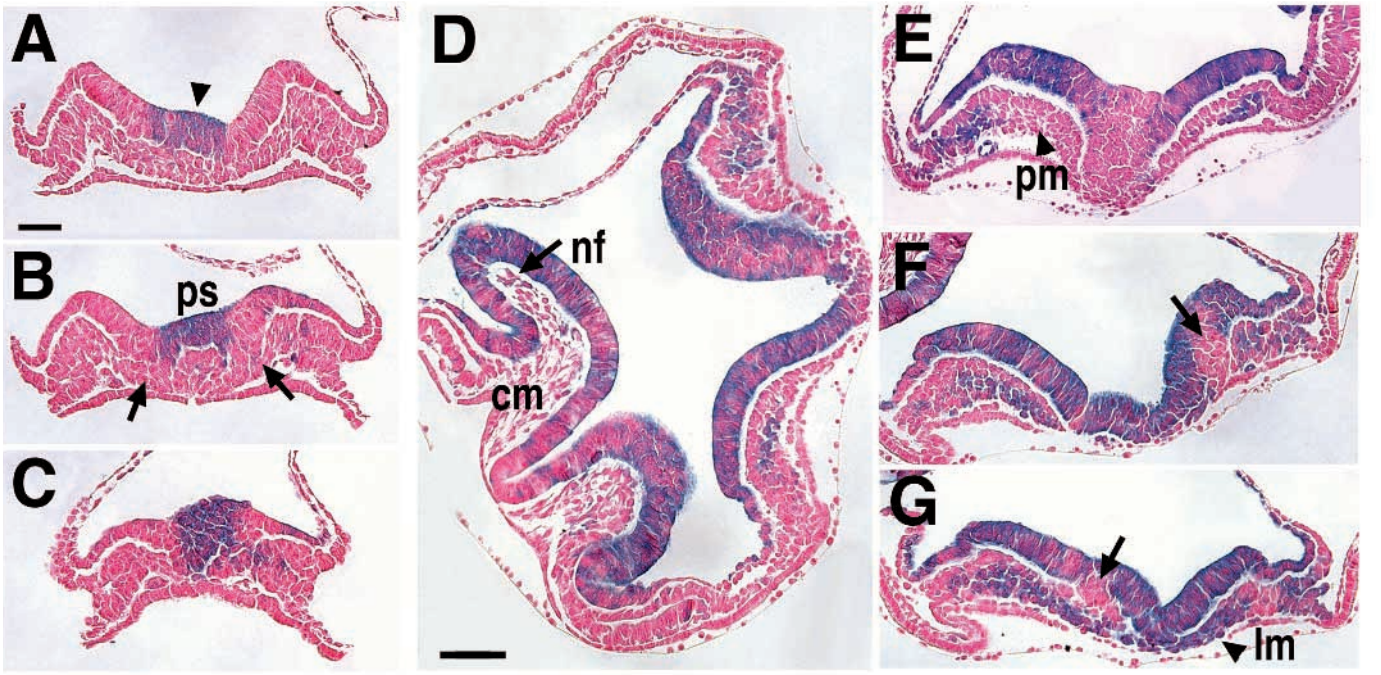

Fig. 8. Histological analysis of whole-mount β-galactosidase stained *fgfr1*$^{\Delta tmk}$/*fgfr1*$^{\Delta tmk}$ ↔ CD-1 chimeras at E8.5. (A-C) Anterior to posterior, transverse sections through the primitive streak of a chimera with minimal *fgfr1*$^{\Delta tmk}$/*fgfr1*$^{\Delta tmk}$ contribution. Sections show the accumulation of *fgfr1*$^{\Delta tmk}$/*fgfr1*$^{\Delta tmk}$ cells within the posterior streak (arrowhead). Mutant cells collect in the epiblast layer while WT cells make an EMT on either side of this *fgfr1*$^{\Delta tmk}$/*fgfr1*$^{\Delta tmk}$ accumulation (arrows). (D) Transverse section through chimera that was approximately 70% *fgfr1*$^{\Delta tmk}$/*fgfr1*$^{\Delta tmk}$ cell-derived; note the deficiency of mutant cells in the cephalic mesoderm, and the misshapen neural folds (arrow). (E-G) Anterior to posterior sections through the caudal end of this chimera showing a lack of mutant cells in the paraxial mesoderm (arrowhead in E), and an accumulation of mutant cells within the posterior epiblast and lateral mesoderm (arrowhead in G). WT cells selectively delaminate from an almost entirely *fgfr1*$^{\Delta tmk}$/*fgfr1*$^{\Delta tmk}$-derived epiblast layer (arrows). Primitive streak (ps), cephalic mesoderm (cm), neural fold (nf), paraxial mesoderm (pm), lateral mesoderm (lm). Scale bars, 50 μm.

FGFR1 in the formation of paraxial mesoderm, we argue that the primary defect associated with the *fgfr1*$^{\Delta tmk}$ mutation is a general deficiency in the ability of epiblast cells to traverse the primitive streak. Although secondary roles for *Fgfr1* in cell survival or proliferation cannot be discounted, they alone do not seem sufficient to explain the absence of *fgfr1*$^{\Delta tmk}$/*fgfr1*$^{\Delta tmk}$ cells from anterior mesoderm and endodermal lineages at the time of their inception.

Defects in migration and cell adhesion are associated with the *fgfr1*$^{\Delta tmk}$ mutation

In addition to showing deficiencies in EMT at gastrulation, *Fgfr1* mutant cells that managed to progress through the primitive streak tended to accumulate along the posterior midline. This aberrant morphogenetic movement of *Fgfr1* mutant cells in *fgfr1*$^{\Delta tmk}$/*fgfr1*$^{\Delta tmk}$ ↔ CD-1 chimeras could be the result of defects in cell adhesion and/or cell migration. Cell-extracellular matrix (ECM) interactions are necessary for cell migration, and mouse embryos homozygous for mutations in *fibronectin* (a glycoprotein component of the ECM) and in *focal adhesion kinase* (a non-receptor protein tyrosine kinase thought to mediate integrin signaling) both show phenotypes remarkably similar to homozygous *fgfr1*$^{\Delta tmk}$ embryos (George et al., 1993; Furuta et al., 1995). Interestingly, chimeric analyses of *T* (*Brachyury*) gene function have also shown accumulations of *T/T* cells at the posterior end of the embryo. *T/T* cells were able to traverse the streak, but the nascent *T/T* mesodermal cells accumulated beneath the primitive streak thus suggesting a role for *T* in regulating the morphogenetic behaviour or adhesive properties of nascent mesoderm (Wilson et al., 1993, 1995). Although the similarity between *T* and *Fgfr1* mutant cell behaviour in chimeric embryos lends credence to the Brachyury-FGF regulatory pathway which has been established in *Xenopus* (Isaacs et al., 1994), homozygous *fgfr1*$^{\Delta tmk}$ embryos continue to express *T* and no changes in *T* expression were observed in *fgfr1*$^{\Delta tmk}$/*fgfr1*$^{\Delta tmk}$ ↔ CD-1 chimeras.

A role for FGFR signaling in cell migration has been established by mutational analyses in other organisms (Reichman-Fried et al., 1994; DeVore et al., 1995). In particular, recent mutations of the *Drosophila* FGF-R2 gene, *heartless* (*htl*), have demonstrated phenotypes strikingly similar to those observed in this study: invaginated mesodermal cells remain aggregated along the ventral midline and fail to migrate in a dorsolateral direction (Gisselbrecht et al., 1996; Beiman et al., 1996). Because these muscle progenitors fail to acquire position-specific inductive cues, *heartless* embryos show a reduction in cardiac, visceral and dorsal somatic muscle fates. However, *htl* mesodermal precursors remain competent to receive inductive signals, and mesodermal fates can be rescued by ectopically expressed decapentaplegic protein (Gisselbrecht et al., 1996; Beiman et al., 1996). This is analogous to the results obtained in our *Fgfr1* chimeric analysis which demonstrate that mutant *Fgfr1* cells can still make all types of mesoderm, but fail to

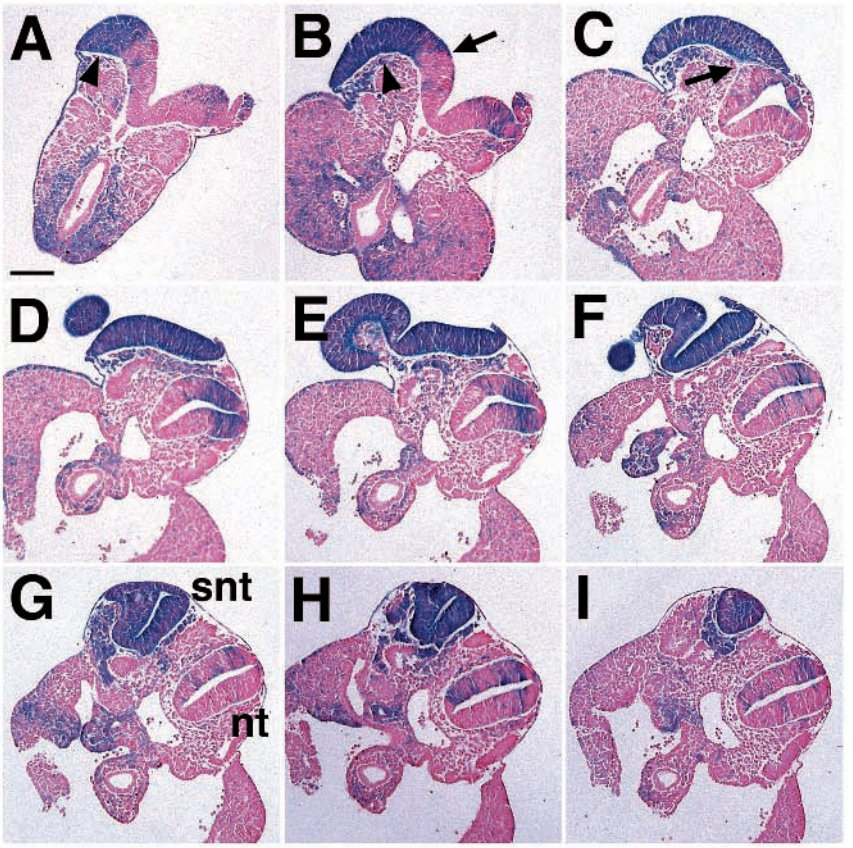

Fig. 9. Progressive caudal to rostral transverse sections through the caudal end of a *fgfr1*$^{\Delta tmk}$/*fgfr1*$^{\Delta tmk}$ ↔ CD-1 chimera at E9.5. Secondary neural tubes begin as a lateral extension of the neural plate (arrowheads in A,B). The ectopic neural plate is excluded from the primary neural tube (C,D), and folds separately into a distinct secondary neural tube (E-I). Note the sharp distinction made between *fgfr1*$^{\Delta tmk}$/*fgfr1*$^{\Delta tmk}$ and WT cells upon primary neural tube closure (arrows in B,C), and the absence of WT cells from the secondary neural tube. Neural tube (nt), secondary neural tube (snt). Scale bar, 100 μm.

migrate properly through the primitive streak. Therefore, there may be a conserved role for FGFR signaling in the morphogenesis of mesoderm formation at gastrulation.

Defects in traversing the primitive streak could also involve altered adhesive properties of *fgfr1*$^{\Delta tmk}$/*fgfr1*$^{\Delta tmk}$ cells. Mutant cells which accumulated within the streak of *fgfr1*$^{\Delta tmk}$/*fgfr1*$^{\Delta tmk}$ ↔ CD-1 chimeras maintained a columnar epithelial morphology, indicating that *fgfr1*$^{\Delta tmk}$/*fgfr1*$^{\Delta tmk}$ cells were failing to

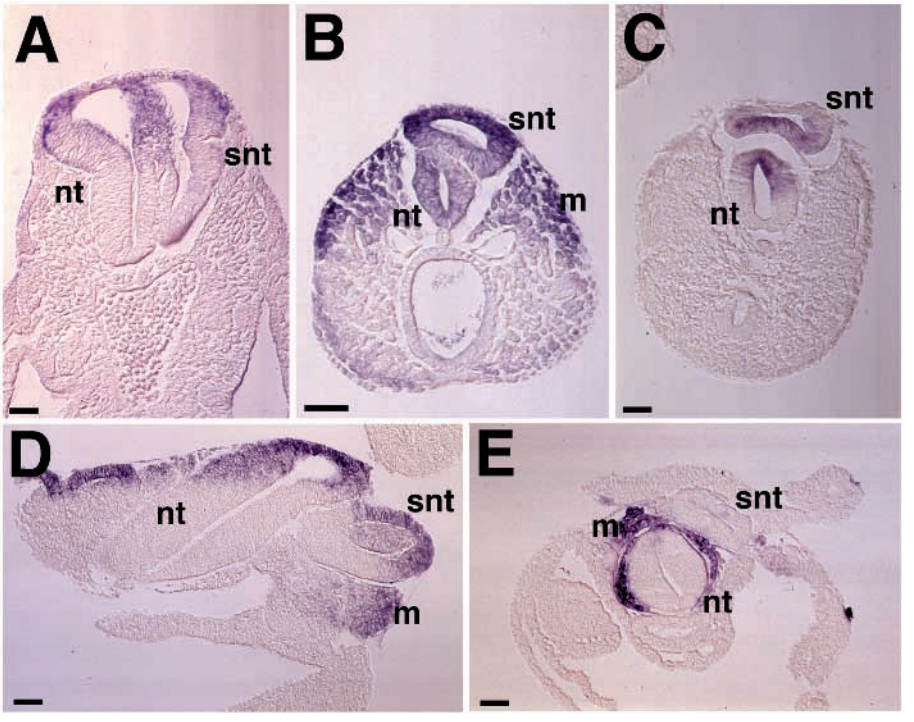

Fig. 10. In situ hybridization analysis of secondary neural tubes from *fgfr1*$^{\Delta tmk}$/*fgfr1*$^{\Delta tmk}$ ↔ CD-1 chimeras. (A) *Sox-1* staining is observed in the dorsal region of both primary and secondary neural tubes. (B) *Ncam* expression is present in both neural tubes in the tail of a *fgfr1*$^{\Delta tmk}$/*fgfr1*$^{\Delta tmk}$ ↔ CD-1 chimera, as well as in the pre-somitic mesoderm. (C) *Pax-6* expression is observed within both primary and secondary neural tubes. (D) *Pax-3* expression is observed in its normal dorsal domain within the primary and secondary neural tubes, as well as in surrounding somitic mesoderm. (E) *Mox-1* is expressed in the poorly organized mesenchyme surrounding primary and secondary neural tubes. Neural tube (nt), secondary neural tube (snt), paraxial mesoderm (m). Scale bars, 50 μm.

fully undergo an epithelial to mesenchymal transition (EMT). EMT events are thought to be regulated by a family of calcium dependent cell adhesion molecules (the cadherins). E-cadherin, for example, is expressed in all cells of the early egg cylinder but is down-regulated at gastrulation within the primitive streak and nascent mesodermal populations (Damjanov et al., 1986). Burdsal et al. (1993) have shown that function perturbing antibodies against E-cadherin can force an EMT in cultured epiblast tissue: epiblast cells lose cell-cell contacts, flatten and assume a mesenchymal morphology. Therefore, there appears to be a causal relationship between loss of cadherin function and EMT. FGFR1 may regulate the expression or function of these adhesion molecules. Indeed, exogenous FGF has been shown to cause mesenchymal transformation of cultured epithelial cell lines (Boyer et al., 1992), and this FGF induced EMT has been associated with the cellular redistribution of E-cadherin. There is also some evidence that cell adhesion molecules may act upstream of FGF signaling by binding to and activating FGF receptors (reviewed by Green et al., 1996). Further study will be needed to determine the relationship between FGFR1 signaling and regulation of cell adhesion at gastrulation.

Neuralization of *fgfr1*$^{\Delta tmk}$/*fgfr1*$^{\Delta tmk}$ cells: morphogenetic movement and cell fate determination

Secondary neural tubes, which are composed entirely of *Fgfr1* mutant cells, form within the posterior trunk and tail of *fgfr1*$^{\Delta tmk}$/*fgfr1*$^{\Delta tmk}$ ↔ CD-1 chimeric embryos. They find their origins from expanded, *fgfr1*$^{\Delta tmk}$/*fgfr1*$^{\Delta tmk}$ cell-derived neural plates which extend laterally from the neural groove and which presumably arise from the accumulation of mutant columnar epithelial cells observed earlier in the streak. Interestingly, these *fgfr1*$^{\Delta tmk}$/*fgfr1*$^{\Delta tmk}$ cells adopt a neural over an epidermal fate. Studies in *Xenopus* have led to the proposal that neuralization of embryonic cells occurs when cells do not receive other inducing signals telling them to form epidermis, mesoderm, or endoderm (for review see Hemmati-Brivanlou and Melton, 1997). The formation of ectopic neural tissue by *fgfr1*$^{\Delta tmk}$/*fgfr1*$^{\Delta tmk}$ cells may therefore demonstrate a similar neuronal default state for murine embryonic cells.

The formation of secondary neural tubes may be a common manifestation of disrupted morphogenesis at gastrulation: duplicated neural tubes have been observed in a number of spontaneously occurring mouse mutations which show defects in primitive streak formation and axis elongation. These mutations include *fused*, *vestigial tail* (*vt*), and *rib vertebrae* (as reviewed by Cogliatti, 1986; Gruneberg and Wickramaratne, 1974; Theiler and Varnum, 1985). Recently, *vt* has been shown to be a hypomorphic allele of *Wnt-3a* (Greco et al., 1996). *Wnt-3a* null mutant embryos lack caudal somites, have disrupted notochord and fail to form a tail bud (Takada et al., 1994). In addition, secondary neural tubes are formed, but, unlike *Fgfr1* mutants, these tubes form from cells that have successfully traversed the streak (Yoshikawa et al., 1997). This has led Yoshikawa et. al. (1997) to propose that *Wnt-3a* regulates the choice of cell fate between neural and paraxial mesodermal cell lineages.

Interestingly, FGFR1 does not appear to be directly required for cell fate specification, yet mutations affecting this pathway can result in similar neural anomalies. Hence, while FGFR1 and Wnt-3a may be playing different roles in the movement and specification of mesodermal progenitors at the primitive streak, disturbances in both systems result in similar phenotypic abnormalities. This study therefore underscores both the complexity of interactions which regulate mesoderm formation, and the importance of normal morphogenetic movements in the processes of patterning and fate determination.

We are grateful to Drs Robin Lovell-Badge and Cynthia Faust for providing the *Sox-1* and *Sox-2*, and the *Ncam* cDNA probes, respectively. We also thank Drs J. Klingensmith, J. Partanen, and J. Pearce for critically reading the manuscript. J. R. is a Terry Fox Research Scientist of the National Cancer Institute of Canada and an International Research Scholar of the Howard Hughes Medical Institute, and B. G. C. is a Scholar of the Natural Sciences and Engineering Research Council of Canada. This work was supported by a program project from the NCIC with funds from the Terry Fox Foundation.

REFERENCES

Amaya, E., Musci, T. J. and Kirschner, M. W. (1991). Expression of a dominant negative mutant of the FGF receptor disrupts mesoderm formation in Xenopus embryos. *Cell* **66,** 257-70.

Amaya, E., Stein, P. A., Musci, T. J. and Kirschner, M. W. (1993). FGF signalling in the early specification of mesoderm in *Xenopus*. *Development* **118,** 477-87.

Beddington, R. S., Puschel, A. W. and Rashbass, P. (1992). Use of chimeras to study gene function in mesodermal tissues during gastrulation and early organogenesis. *Ciba Found. Symp.* **165,** 61-74; discussion 74-7.

Beddington, R. S. (1994). Induction of a second neural axis by the mouse node. *Development* **120,** 613-20.

Beiman, M., Shilo, B. Z. and Volk, T. (1996). Heartless, a Drosophila FGF receptor homolog, is essential for cell migration and establishment of several mesodermal lineages. *Genes Dev.* **10,** 2993-3002.

Boyer, B., Dufour, S. and Thiery, J. P. (1992). E-cadherin expression during the acidic FGF-induced dispersion of a rat bladder carcinoma cell line. *Exp. Cell Res.* **201,** 347-57.

Burdsal, C. A., Damsky, C. H. and Pedersen, R. A. (1993). The role of E-cadherin and integrins in mesoderm differentiation and migration at the mammalian primitive streak. *Development* **118,** 829-44.

Candia, A. F., Hu, J., Crosby, J., Lalley, P. A., Noden, D., Nadeau, J. H. and Wright, C. V. (1992). Mox-1 and Mox-2 define a novel homeobox gene subfamily and are differentially expressed during early mesodermal patterning in mouse embryos. *Development* **116,** 1123-36.

Cogliatti, S. B. (1986). Diplomyelia: caudal duplication of the neural tube in mice. *Teratology* **34,** 343-52.

Collignon, J., Sockanathan, S., Hacker, A., Cohen-Tannoudji, M., Norris, D., Rastan, S., Stevanovic, M., Goodfellow, P. N. and Lovell-Badge, R. (1996). A comparison of the properties of Sox-3 with Sry and two related genes, Sox-1 and Sox-2. *Development* **122**, 509-520.

Conlon, R. A. and Rossant, J. (1992). Exogenous retinoic acid rapidly induces anterior ectopic expression of murine *Hox-2* genes in vivo. *Development* **116,** 357-68.

Cox, W. G. and Hemmati-Brivanlou, A. (1995). Caudalization of neural fate by tissue recombination and bFGF. *Development* **121,** 4349-4358.

Damjanov, I., Damjanov, A. and Damsky, C. H. (1986). Developmentally regulated expression of the cell-cell adhesion glycoprotein cell-CAM 120/80 in peri-implantation mouse embryos and extraembryonic membranes. *Dev. Biol.* **116,** 194-202.

Deng, C. X., Wynshaw-Boris, A., Shen, M. M., Daugherty, C., Ornitz, D. M. and Leder, P. (1994). Murine FGFR-1 is required for early postimplantation growth and axial organization. *Genes Dev.* **8,** 3045-3057.

DeVore, D. L., Horvitz, H. R. and Stern, M. J. (1995). An FGF receptor signaling pathway is required for the normal cell migrations of the sex myoblasts in C. elegans hermaphrodites. *Cell* **83,** 611-620.

Echelard, Y., Epstein, D. J., St-Jacques, B., Shen, L., Mohler, J., McMahon, J. A. and McMahon, A. P. (1993). Sonic hedgehog, a member of a family of putative signaling molecules, is implicated in the regulation of CNS polarity. *Cell* **75,** 1417-30.

Feldman, B., Poueymirou, W., Papaioannou, V. E., DeChiara, T. M. and Goldfarb, M. (1995). Requirement of FGF-4 for postimplantation mouse development. *Science* **267,** 246-249.

Friedrich, G. and Soriano, P. (1991). Promoter traps in embryonic stem cells: a genetic screen to identify and mutate developmental genes in mice. *Genes Dev*. **5,** 1513-23.

Furuta, Y., Ilic, D., Kanazawa, S., Takeda, N., Yamamoto, T. and Aizawa, S. (1995). Mesodermal defect in late phase of gastrulation by a targeted mutation of focal adhesion kinase, FAK. *Oncogene* **11,** 1989-1995.

George, E. L., Georges-Labouesse, E. N., Patel-King, R. S., Rayburn, H. and Hynes, R. O. (1993). Defects in mesoderm, neural tube and vascular development in mouse embryos lacking fibronectin. *Development* **119,** 1079-91.

Gisselbrecht, S., Skeath, J. B., Doe, C. Q. and Michelson, A. M. (1996). heartless encodes a fibroblast growth factor receptor (DFR1/DFGF-R2) involved in the directional migration of early mesodermal cells in the Drosophila embryo. *Genes Dev.* **10,** 3003-3017.

Givol, D. and Yayon, A. (1992). Complexity of FGF receptors: genetic basis for structural diversity and functional specificity. *Faseb J.* **6,** 3362-9.

Goulding, M. D., Chalepakis, G., Deutsch, U., Erselius, J. R. and Gruss, P. (1991). Pax-3, a novel murine DNA binding protein expressed during early neurogenesis. *EMBO J.* **10,** 1135-47.

Greco, T. L., Takada, S., Newhouse, M. M., McMahon, J. A., McMahon, A. P. and Camper, S. A. (1996). Analysis of the vestigial tail mutation demonstrates that Wnt-3a gene dosage regulates mouse axial development. *Genes Dev.* **10,** 313-324.

Green, P. J., Walsh, F. S. and Doherty, P. (1996). Promiscuity of fibroblast growth factor receptors. *BioEssays* **18,** 639-646.

Gruneberg, H. and Wickramaratne, G. A. (1974). A re-examination of two skeletal mutants of the mouse, vestigial-tail (vt) and congenital hydrocephalus (ch). *J. Embryol. Exp. Morphol.* **31,** 207-22.

Haub, O. and Goldfarb, M. (1991). Expression of the fibroblast growth factor-5 gene in the mouse embryo. *Development* **112,** 397-406.

Hebert, J. M., Boyle, M. and Martin, G. R. (1991). mRNA localization studies suggest that murine FGF-5 plays a role in gastrulation. *Development* **112,** 407-15.

Hebert, J. M., Rosenquist, T., Gotz, J. and Martin, G. R. (1994). FGF5 as a regulator of the hair growth cycle: evidence from targeted and spontaneous mutations. *Cell* **78,** 1017-1025.

Hemmati-Brivanlou, A. and Melton, D. A. (1997). Vertebrate embryonic cells will become nerve cells unless told otherwise. *Cell* **88,** 13-17.

Herrmann, B. G. (1991). Expression pattern of the Brachyury gene in whole-mount TWis/TWis mutant embryos. *Development* **113,** 913-917.

Hogan, B., Beddington, R., Costantini, F. and Lacy, E. (1994). *Manipulating the Mouse Embryo. A Laboratory Manual*. Second edition. Cold Spring Harbor Laboratory Press, New York.

Isaacs, H. V., Pownall, M. E. and Slack, J. M. W. (1994). eFGF regulates Xbra expression during Xenopus gastrulation. *EMBO J.* **13**, 4469-4481.

Kengaku, M. and Okamoto, H. (1995). bFGF as a possible morphogen for the anteroposterior axis of the central nervous system in *Xenopus. Development* **121,** 3121-3130.

Kimelman, D. and Kirschner, M. (1987). Synergistic induction of mesoderm by FGF and TGF-beta and the identification of an mRNA coding for FGF in the early Xenopus embryo. *Cell* **51,** 869-77.

Kroll, K. L. and Amaya, E. (1996). Transgenic Xenopus embryos from sperm nuclear transplantations reveal FGF signaling requirements during gastrulation. *Development* **122,** 3173-3183.

Lamb, T. M. and Harland, R. M. (1995). Fibroblast growth factor is a direct neural inducer, which combined with noggin generates anterior-posterior neural pattern. *Development* **121,** 3627-3636.

Lawson, K. A., Meneses, J. J. and Pedersen, R. A. (1991). Clonal analysis of epiblast fate during germ layer formation in the mouse embryo. *Development* **113,** 891-911.

Mansour, S. L., Goddard, J. M. and Capecchi, M. R. (1993). Mice homozygous for a targeted disruption of the proto-oncogene int-2 have developmental defects in the tail and inner ear. *Development* **117,** 13-28.

McWhir, J., Schnieke, A. E., Ansell, R., Wallace, H., Colman, A., Scott, A. R. and Kind, A. J. (1996). Selective ablation of differentiated cells permits isolation of embryonic stem cell lines from murine embryos with a non-permissive genetic background. *Nat. Genet.* **14,** 223-226.

Nagy, A., Rossant, J., Nagy, R., Abramow-Newerly, W. and Roder, J. C. (1993). Derivation of completely cell culture-derived mice from early-passage embryonic stem cells. *Proc. Natl. Acad. Sci. USA* **90,** 8424-2428.

Nicolas, J. F., Mathis, L., Bonnerot, C. and Saurin, W. (1996). Evidence in the mouse for self-renewing stem cells in the formation of a segmented longitudinal structure, the myotome. *Development* **122,** 2933-2946.

Niswander, L. and Martin, G. R. (1992). Fgf-4 expression during gastrulation, myogenesis, limb and tooth development in the mouse. *Development* **114,** 755-768.

Ornitz, D. M., Xu, J., Colvin, J. S., McEwen, D. G., MacArthur, C. A., Coulier, F., Gao, G. and Goldfarb, M. (1996). Receptor specificity of the fibroblast growth factor family. *J. Biol. Chem.* **271,** 15292-15297.

Orr-Urtreger, A., Givol, D., Yayon, A., Yarden, Y. and Lonai, P. (1991). Developmental expression of two murine fibroblast growth factor receptors, flg and bek. *Development* **113,** 1419-1434.

Parameswaran, M. and Tam, P. P. (1995). Regionalisation of cell fate and morphogenetic movement of the mesoderm during mouse gastrulation. *Dev. Genet.* **17,** 16-28.

Paterno, G. D., Gillespie, L. L., Dixon, M. S., Slack, J. M. and Heath, J. K. (1989). Mesoderm-inducing properties of INT-2 and kFGF: two oncogene-encoded growth factors related to FGF. *Development* **106,** 79-83.

Pownall, M. E., Tucker, A. S., Slack, J. M. and Isaacs, H. V. (1996). eFGF, Xcad3 and Hox genes form a molecular pathway that establishes the anteroposterior axis in *Xenopus*. *Development* **122,** 3881-3892.

Reichman-Fried, M., Dickson, B., Hafen, E. and Shilo, B. Z. (1994). Elucidation of the role of breathless, a Drosophila FGF receptor homolog, in tracheal cell migration. *Genes Dev.* **8,** 428-439.

Slack, J. M., Darlington, B. G., Gillespie, L. L., Godsave, S. F., Isaacs, H. V. and Paterno, G. D. (1989). The role of fibroblast growth factor in early *Xenopus* development. *Development* **107 Suppl,** 141-148.

Smith, D. E., Franco del Amo, F. and Gridley, T. (1992). Isolation of *Sna*, a mouse gene homologous to the *Drosophila* genes *snail* and *escargot*: its expression pattern suggests multiple roles during postimplantation development. *Development* **116,** 1033-1039.

Takada, S., Stark, K. L., Shea, M. J., Vassileva, G., McMahon, J. A. and McMahon, A. P. (1994). Wnt-3a regulates somite and tailbud formation in the mouse embryo. *Genes Dev*. **8,** 174-189.

Tam, P. P. and Beddington, R. S. (1987). The formation of mesodermal tissues in the mouse embryo during gastrulation and early organogenesis. *Development* **99,** 109-126.

Tam, P. P. (1989). Regionalisation of the mouse embryonic ectoderm: allocation of prospective ectodermal tissues during gastrulation. *Development* **107,** 55-67.

Theiler, K. and Varnum, D. S. (1985). Development of rib-vertebrae: a new mutation in the house mouse with accessory caudal duplications. *Anat. Embryol.* **173,** 111-6.

Walther, C. and Gruss, P. (1991). Pax-6, a murine paired box gene, is expressed in the developing CNS. *Development* **113,** 1435-49.

Wilkinson, D. G., Peters, G., Dickson, C. and McMahon, A. P. (1988). Expression of the FGF-related proto-oncogene int-2 during gastrulation and neurulation in the mouse. *EMBO J.* **7,** 691-5.

Wilson, V., Rashbass, P. and Beddington, R. S. (1993). Chimeric analysis of T (Brachyury) gene function. *Development* **117,** 1321-31.

Wilson, V., Manson, L., Skarnes, W. C. and Beddington, R. S. (1995). The T gene is necessary for normal mesodermal morphogenetic cell movements during gastrulation. *Development* **121,** 877-886.

Wolf, C., Thisse, C., Stoetzel, C., Thisse, B., Gerlinger, P. and Perrin-Schmitt, F. (1991). The M-twist gene of Mus is expressed in subsets of mesodermal cells and is closely related to the Xenopus X-twi and the Drosophila twist genes. *Dev. Biol.* **143,** 363-73.

Yamaguchi, T. P., Conlon, R. A. and Rossant, J. (1992). Expression of the fibroblast growth factor receptor FGFR-1/flg during gastrulation and segmentation in the mouse embryo. *Dev. Biol.* **152,** 75-88.

Yamaguchi, T. P., Harpal, K., Henkemeyer, M. and Rossant, J. (1994). fgfr-1 is required for embryonic growth and mesodermal patterning during mouse gastrulation. *Genes Dev*. **8,** 3032-3044.

Yoshikawa, Y., Fujimori, T., McMahon, A. P. and Takada, S. (1997). Evidence that absence of Wnt-3a signaling promotes neuralization instead of paraxial mesoderm development in the mouse. *Dev. Biol*. **183**, 234-242.

(Accepted 9 May 1997)